ERMAKOV, YE. V. On the mechanism of developing astheno-vegetative disturbance nder the chronic effect of a SHF-field, *Voyenno-Medit. Zh. (USSR), 3:* 42, 1969.

ABLUBOVSKAYA, N. P. Reactions of living organisms to exposure to millimeter-band lectromagnetic waves. *Trans. Usp. Fiz. Nauk. 110:* 574–575, 1973.

ARET, M. M., CLEARY, S., PASTERNACK, B., EISENBUD, M. AND SCHMIDT, H. *A Study of enticular Imperfections in the Eyes of a Sample of Microwave Workers and a Control opulation.* New York University, New York Final Rep. RADC-TDR-63-124, ASTIA oc. AD 413-294, 1963.

ARET, M. M., KAPLAN, I. T. AND KAY, A. M. Clinical microwave cataracts. *In: Biologic ffects and Health Implications of Microwave Radiation.* Cleary, S. (Ed). USDHEW, HS, BRH/DBE 70-2, p. 82, 1970.

8

Biophysics of Ultrasound

LEON A. FRIZZELL
FLOYD DUNN[1]

Introduction

Ultrasound is acoustic energy beyond the audible range (*viz.*, frequencies above 20 kHz). This form of energy is used extensively in medical diagnosis as well as in therapeutic applications. In this chapter, a) the physical characteristics of ultrasonic fields are presented, including discussion of the acoustic variables; b) information is provided on ultrasonic sources and measurement methods; and c) ultrasonic propagation in, and interaction with, tissues is described. It was considered essential to include the mathematical expressions which relate the various acoustic field variables and quantities which characterize the state of a system for a quantitative understanding of ultrasonic methods. While these equations are discussed in sufficient detail to be used to compute quantities of interest, their derivations have not been included. Readers desiring a deeper knowledge of the origin of these expressions are urged to consult the references provided. For the purpose of this discussion, only infinitesimal amplitude (linearized relations) acoustic disturbances are presented.

Physical Characteristics of Ultrasonic Fields

Initial discussion of acoustic relationships and transmission phenomena is confined to plane acoustic waves, *i.e.*, those for which the wave fronts are plane surfaces. More complex beam profiles originating from typical unfocused sources and focusing systems are discussed later.

FUNDAMENTAL ACOUSTIC RELATIONSHIPS

The fundamental acoustic relationships are the same whether ultrasound or audible sound is discussed. For either, changes occur in a number of

[1] The authors acknowledge gratefully support for the portions of the work, described in this chapter, accomplished at this laboratory in recent years, by the National Institutes of Health and the National Science Foundation.

physical variables which describe the state of a system or medium. Changes occur, for example, in the pressure and density of an elastic medium in which an acoustic field exists. For a sinusoidal plane traveling wave (traveling in the positive direction of the x-axis) with no attenuation of acoustic energy occurring in the medium (*i.e.*, no loss of energy from the waves as they travel along the x-axis), the changes in each of these (and other) physical parameters can be expressed as follows for the "linear range":

$$m = M \cos \omega(t - x/c) \tag{1}$$

where m designates any one of the variables which undergoes change during the presence of the disturbance in the medium, and M is the amplitude of the cyclic changes in the variable. The quantity c is the free field sound velocity for the medium (the speed with which a plane wave disturbance propagates in a medium of infinite extent); t and x are the time and space variables, respectively; and ω is the angular frequency, which is equal to $2\pi f$, where f is the frequency.

That Equation *1* describes a wave traveling in the positive x-direction is apparent upon examination of the argument of the cosine function. The argument is a constant when a time increase by an amount Δt is coupled with a positive shift in distance of $\Delta x = c\Delta t$ (see Figure 8.1*a*). It is equally apparent that if the minus sign in the argument of the cosine function were made a plus sign, Equation *1* would describe a wave traveling in the negative x-direction.

Acoustic propagation is characterized by adiabatic changes in the state of the medium; that is, heat transfer does not occur to any great extent during the changes in pressure. It follows, therefore, that the free field velocity can be expressed as

$$c = \sqrt{\frac{1}{\rho_0 K_{ad}}} \tag{2}$$

where ρ_0 designates the undisturbed density of the medium (density of the medium in the absence of an acoustic disturbance); and K_{ad} designates its adiabatic compressibility (1). That is, for the linearized case (small amplitude acoustical disturbances) with negligible absorption, the velocity of acoustic wave transmission is independent of frequency and amplitude, and is determined solely by the density and adiabatic compressibility of the medium. Hence, waves of arbitrary shape travel without change in form.

In the presence of an acoustic wave, the molecules of a liquid and the particles of other materials in the liquid undergo periodic excursions from their undisturbed positions, termed the particle displacement. The amplitudes of the resulting particle velocity and particle acceleration, which are the first and second time derivatives of displacement, respectively, depend upon the amplitude of this excursion and the frequency of the acoustic waves. The frequency is equal to the reciprocal of the period τ of the wave

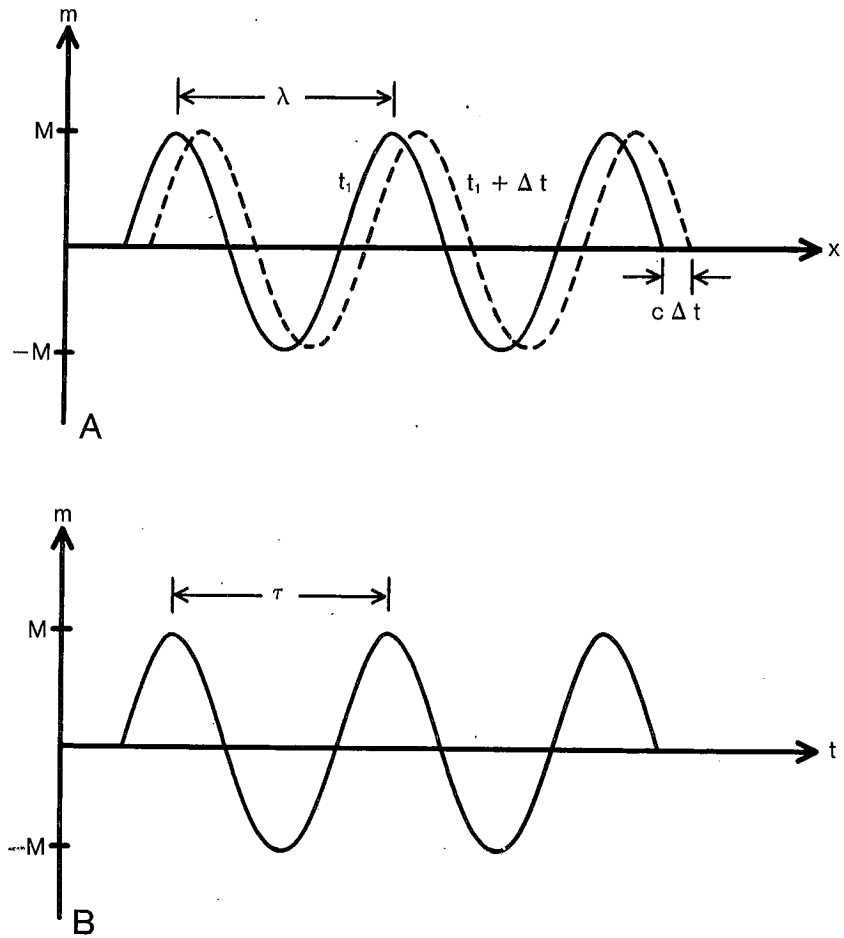

Fig. 8.1. (*a*) Instantaneous spatial distribution of a sinusoidally varying acoustic field variable at two instants of time. (*b*) Temporal distribution of an acoustic variable at a specific point in the field.

(see Figure 8.1*b*). The wavelength λ, which is defined by the relationship

$$c = f\lambda \tag{3}$$

is the distance separating adjacent planes of equal phase, *e.g.*, the distance from crest to crest (see Figure 8.1*a*). The interaction of ultrasound and biological systems may involve any of a number of physical parameters which undergo changes in the field. It is, therefore, desirable to summarize the relationships between the more important parameters. For a plane traveling wave, the variations in pressure, particle velocity and particle acceleration all satisfy Equation *1*, where m designates any one of the parameters and M designates its amplitude. The relationships between the

TABLE 8.1 *Relationships Between Amplitudes of Acoustic Parameters*[a]

Parameter	Parameter Symbol	Amplitude Symbol	P (Pa)[b]	D (m)	U (m/s)	A (m/s^2)	I (W/m^2)
Acoustic Pressure	p	P	± 1	$\pm j\omega\rho_0 c$	$\pm\rho_0 c$	$\pm\frac{\rho_0 c}{j\omega}$	$\pm\sqrt{2\rho_0 cI}\,\frac{1}{I}$
Particle Displacement	ξ	D	$\pm\frac{1}{j\omega\rho_0 c}$	$\mp\!\!\mp 1$	$\mp\!\!\mp\frac{1}{j\omega}$	$=\frac{1}{\omega^2}$	$\mp\!\!\mp\sqrt{\frac{2I}{\rho_0 c\omega^2}}\,\frac{1}{I}$
Particle Velocity	$\dot{\xi}$	U	$\pm\frac{1}{\rho_0 c}$	$\mp\!\!\mp j\omega$	$\mp\!\!\mp 1$	$\mp\!\!\mp\frac{1}{j\omega}$	$\pm\sqrt{\frac{2I}{\rho_0 c}}\,\frac{1}{I}$
Particle Acceleration	$\ddot{\xi}$	A	$\pm\frac{j\omega}{\rho_0 c}$	$\mp\!\!\mp\omega^2$	$\mp\!\!\mp j\omega$	$\mp\!\!\mp 1$	$\mp\!\!\mp\sqrt{\frac{2\omega^2 I}{\rho_0 c}}\,\frac{1}{I}$
Intensity	I	I	$\mp\!\!\mp\frac{1}{2}\frac{P}{\rho_0 c}$	$\mp\!\!\mp\frac{1}{2}\rho_0 c\omega^2$	$\mp\!\!\mp\frac{1}{2}\rho_0 cU$	$\mp\!\!\mp\frac{1}{2}\frac{\rho_0 c}{\omega^2}A$	$\mp\!\!\mp 1$

[a] Multiply expressions in table by column heading to obtain the amplitude quantities tabulated in the Amplitude Symbol column. ($j = \sqrt{-1}$). The *upper sign* applies to waves traveling in the positive direction, while the *lower sign* applies to waves traveling in the negative direction.
[b] 1 P_a = 1 N/m^2.

amplitudes of these parameters are listed in Table 8.1, where all quantities are expressed in *SI* units. The symbol $j = \sqrt{-1}$ in Table 8.1 indicates a 90° phase difference. A positive j indicates that the parameter in the left-most column *leads* the parameter in question by 90°, a negative j is associated with a 90° phase *lag*, while a minus sign only indicates 180° in phase difference. The product $\rho_0 c$, which appears in a number of these equations, is defined entirely in terms of constants characteristic of the medium, and is called the characteristic acoustic impedance of the medium. For plane waves in lossless media the specific acoustic impedance, defined as the ratio of the acoustic pressure amplitude to the particle velocity amplitude, is equal to the characteristic acoustic impedance. Impedance ratios are used for determining the reflection at interfaces between media, as discussed later.

The intensity of a sound wave is defined as the time average of the rate of propagation of energy through a unit area normal to the direction of propagation (unit area perpendicular to the x-axis for waves designated by Equation *1*). It is desirable to consider numerical examples to develop a feeling for the magnitudes of the changes which occur in the various physical parameters. Accordingly, some values are listed in Table 8.2. For convenience, the technology of ultrasound developed using a mixed system of units, where intensity is expressed in watts per square centimeter while acoustic pressure amplitude is in atmospheres; this is found throughout the literature. Therefore, the values in Table 8.2 are presented in the more-commonly used units as well as in *SI* units. However, because workers in the field cling to the more commonly used units as being more useful and meaningful, these will be used in the rest of the chapter.

The propagation of a plane traveling wave in an absorbing medium is

TABLE 8.2. *Numerical Examples of Acoustical Parameters for Water. Frequency = 1 MHz, Temperature = 30° C, Ambient pressure = 1 Atm ≃ 10^5 Pa*[a]

Parameter	I	P	D	U	A
For common units of	$\frac{W}{cm^2}$	Atm	cm	cm/s	$\frac{cm}{s^2}$
Multiply figures in table by	1	1	10^{-6}	1	10^6
For SI units of	$\frac{W}{m^2}$	Pa	m	m/s	m/s^2
Multiply figures in table by	10^4	10^5	10^{-8}	10^{-2}	10^4
	0.01	0.171	0.183	1.15	7.22
	1	1.71	1.83	11.5	72.2
	100	17.1	18.3	115	722

[a] 1 Pa = 1 N/m^2

described as

$$m = Me^{-\alpha x}\cos\omega\left(t - \frac{x}{c}\right) \tag{4}$$

where α is the amplitude absorption coefficient, absorption per unit path length. The amplitude $Me^{-\alpha x}$ of the wave decreases exponentially as it progresses in the positive x-direction. The intensity I of a plane progressive wave moving in the positive direction, at any position x in the medium, can be expressed in terms of the intensity I_0 at $x = 0$ as

$$I = I_0 e^{-2\alpha x} \tag{5}$$

Absorption is the conversion of the mechanical energy of an ultrasonic wave into heat. In an inhomogeneous medium (*i.e.*, one whose properties vary with position) other processes occur which may redirect the acoustic energy out of the main beam and prevent its being received by a suitable detector. One such process is the scattering of energy in all directions because of reflections at interfaces of structures which are small compared with the wavelength of sound and which have different acoustic properties from those of the surrounding medium. These processes, including absorption, contribute to the attenuation of the ultrasonic wave as it propagates; their combined effect can be described by an equation such as Equation *5* where an attenuation coefficient is substituted for the absorption coefficient. The absorption coefficient, however, determines the heat generated by the passage of ultrasound through tissue, and is thus of primary importance in ultrasound therapy. The values of the acoustic parameters for tissues will be given later.

Wave phenomena can produce steady forces on interfaces between media which have different values of acoustic velocity and/or density and within homogeneous absorbing media. The radiation force at a plane interface depends on the relative amount of incident energy reflected versus the amount transmitted or absorbed, and is equal to the difference in energy densities in the two media. The energy density E, or total energy per unit volume, of the plane wave is given by

$$E = I/c \tag{6}$$

where I is the acoustic intensity and c is the acoustic velocity. The use of the phenomenon of radiation force to determine total acoustic power and intensity is discussed later in this chapter.

REFLECTION, REFRACTION AND MODE CONVERSION

In order to understand the characteristics of transmission of ultrasound through tissue it is important to be familiar with certain quantitative relationships which describe the reflection and transmission of acoustic waves at boundaries. The amplitudes of waves reflected and/or refracted

(redirection upon transmission past an interface) at an interface between media are determined by the acoustic velocities and densities of the respective media and by the angle at which the wave is incident on the interface.

The acoustic disturbances described by Equation *1* represent unattenuated traveling plane waves. For this type of wave, the magnitude of the change in each physical parameter is the same at all positions in the field. However, if reflection of acoustic energy takes place, the simple traveling wave equation no longer describes the acoustic conditions. Four relevant cases are described:

Case 1: Consider first the case of partial reflection at normal incidence (1), defined by a 90° angle between the direction of the incident wave and the boundary (see Figure 8.2). The acoustic pressure variation in the medium of incidence, Medium 1, can be represented analytically as

$$p = P_+\cos\omega\left(t - \frac{x}{c}\right) + P_-\cos\omega\left(t + \frac{x}{c}\right) \tag{7}$$

where P_+ is the pressure amplitude of the wave traveling in the positive x-direction (the incident wave), and P_- is the pressure amplitude of the wave traveling in the negative x-direction (the reflected wave). The two waves

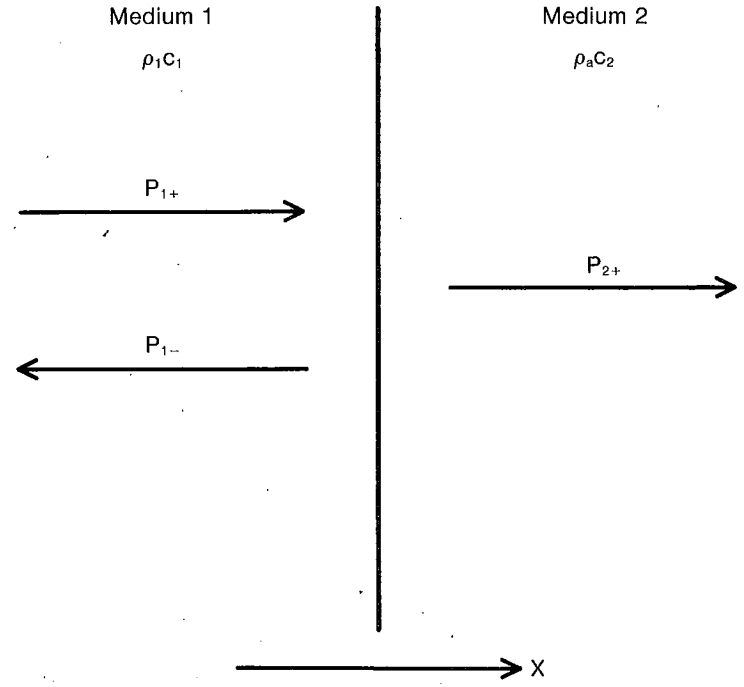

Fig. 8.2. Wave in Medium 1 incident normal to plane interface between Medium 1 and Medium 2. No energy returned to interface in Medium 2 and no absorption within media.

combine to produce a standing wave having maxima and minima of acoustic pressure, and of the other acoustic quantities, at fixed distances from the boundary. The pressure amplitude of the reflected wave P_- is given by the product of the pressure amplitude of the incident wave P_+ and the pressure reflection coefficient R_P which is a function only of the ratio of the characteristic acoustic impedances of the two media,

$r_{21} = \frac{\rho_2 c_2}{\rho_1 c_1}$, as follows

$$R_P = \frac{r_{21} - 1}{r_{21} + 1} \tag{8}$$

The pressure amplitude of the transmitted wave, P_{2+} in Figure 8.2, is given by the product of the pressure amplitude of the incident wave and the pressure transmission coefficient T_p where

$$T_p = \frac{2r_{21}}{1 + r_{21}} \tag{9}$$

It is assumed that there is no reflector or source in Medium 2.

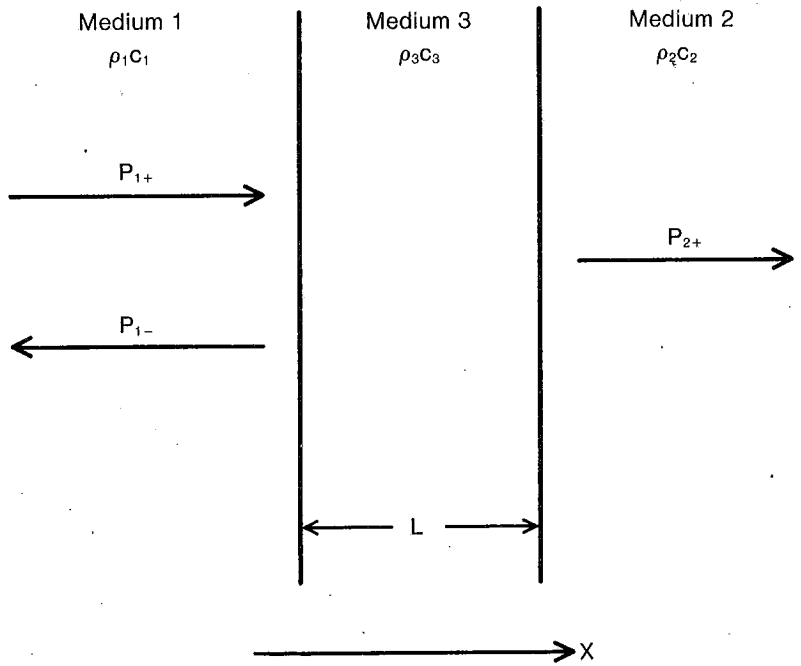

Fig. 8.3. Wave in Medium 1 at normal incidence. Slab of Medium 3 interposed between Medium 1 and Medium 2. No energy returned to interface in Medium 2 and no absorption within media.

The intensity reflection coefficient R_I and the intensity transmission coefficient T_I are given by

$$R_I = R_p^2 = \left[\frac{r_{21} - 1}{r_{21} + 1}\right]^2 \tag{10}$$

$$T_I = T_p^2/r_{21} = \frac{4r_{21}}{(r_{21} + 1)^2} \tag{11}$$

A number of points should be noted from Equations 8 through 11. First, if the impedances are equal in the two media ($r_{21} = 1$), the incident wave is totally transmitted beyond the interface. If $r_{21} > 1$ the pressure amplitude reflected at the interface adds to the incident pressure amplitude, increasing the value at that point in the field. Where $r_{21} < 1$, the opposite effect occurs, and the pressure amplitude at the interface is decreased below that of the incident wave. For the two extremes, $r_{21} = 0$ and $r_{21} = \infty$, all incident energy is reflected (*i.e.*, none is transmitted).

Case 2: Consider normal incidence again, but with a slab of a third medium of thickness L interposed between the two media (see Figure 8.3). The pressure reflection coefficient R_P and the pressure transmission coefficient T_P are functions of the ratios of the characteristic impedances of the three media and of the quantity $\omega L/c_3$ (equal to $2\pi L/\lambda_3$), which is determined by the ratio of the thickness L to the wavelength in Medium 3. For normally incident continuous waves, these coefficients are

$$R_P = \frac{P_{1-}}{P_{1+}} = \left[1 - \frac{4r_{21}}{(r_{21} + 1)^2\cos^2\frac{\omega L}{c_3} + (r_{31} + r_{23})^2\sin^2\frac{\omega L}{c_3}}\right]^{1/2} \tag{12}$$

$$T_P = \frac{P_{2+}}{P_{1+}} = \left[\frac{4r_{21}^2}{(r_{21} + 1)^2\cos^2\frac{\omega L}{c_3} + (r_{31} + r_{23})^2\sin^2\frac{\omega L}{c_3}}\right]^{1/2} \tag{13}$$

where

$$r_{21} = \frac{\rho_2 c_2}{\rho_1 c_1}, \qquad r_{31} = \frac{\rho_3 c_3}{\rho_1 c_1}, \quad \text{and} \quad r_{23} = \frac{\rho_2 c_2}{\rho_3 c_3}$$

The intensity reflection coefficient R_I and the intensity transmission coefficient T_I are given by the following:

$$R_I = R_P^2 = 1 - \frac{4r_{21}}{(r_{21} + 1)^2\cos^2\frac{\omega L}{c_3} + (r_{31} + r_{23})^2\sin^2\frac{\omega L}{c_3}} \tag{14}$$

$$T_I = T_p^2/r_{21} = \frac{4r_{21}}{(r_{21} + 1)^2\cos^2\frac{\omega L}{c_3} + (r_{31} + r_{23})^2\sin^2\frac{\omega L}{c_3}} \tag{15}$$

Several situations are of interest: if the characteristic impedance of Medium 3 is intermediate between those of Media 1 and 2, transmission of energy T_I can be maximized by choosing the thickness L to satisfy the equation

$$L = (2n - 1)\lambda/4, \qquad n = 1, 2, 3, \ldots. \tag{16}$$

The intensity transmission coefficient then becomes

$$T_I = \frac{4r_{21}}{(r_{31} + r_{23})^2} \tag{17}$$

That is, the best choice of thickness for maximum transmission for any interposed material (if its characteristic acoustic impedance is anywhere between the values of the other media) is an odd number of quarter wavelengths. In addition, if it is possible to choose the interposed material so that its characteristic acoustic impedance is optimum for transmitting acoustic energy, the reflected wave in Medium 1 can be completely eliminated by choosing the intermediate material so that

$$\rho_3 c_3 = \sqrt{(\rho_1 c_1)(\rho_2 c_2)} \tag{18}$$

If the characteristic acoustic impedance of Medium 3 is not between those of the other two media, the optimum choice of thickness for the slab (to obtain the maximum value of the transmission coefficient) is an integral multiple of a half-wavelength (*i.e.*, $L = n\lambda/2$, $n = 1, 2, 3, \ldots$). The transmission coefficient then becomes the same as that for Case 1.

If Media 1 and 2 have nearly equal characteristic acoustic impedances, and if the thickness of the interposed slab satisfies

$$L \leq \frac{\lambda}{20\pi r_{31}} \tag{19}$$

then the transmission coefficient will not differ from that of Case 1 by more than one percent, *i.e.*, Medium 3 acts largely as a transparent acoustic window. If the characteristic acoustic impedance of Medium 3 is less than that of Media 1 and 2, r_{23} should be used in place of r_{31} in Equation 19.

Case 3: A plane wave is incident at any angle θ_1 to the normal of the plane interface between two media (see Figure 8.4). The angle of refraction θ_2 is a function of the angle of incidence and the ratio of the velocity of sound in the two media as follows

$$\sin\theta_2 = \frac{c_2}{c_1}\sin\theta_1 \tag{20}$$

and the angle of reflection is equal to the angle of incidence. The pressure transmission and reflection coefficients, and the intensity transmission and reflection coefficients, further involve the ratio of the characteristic impedances as shown in the following equations:

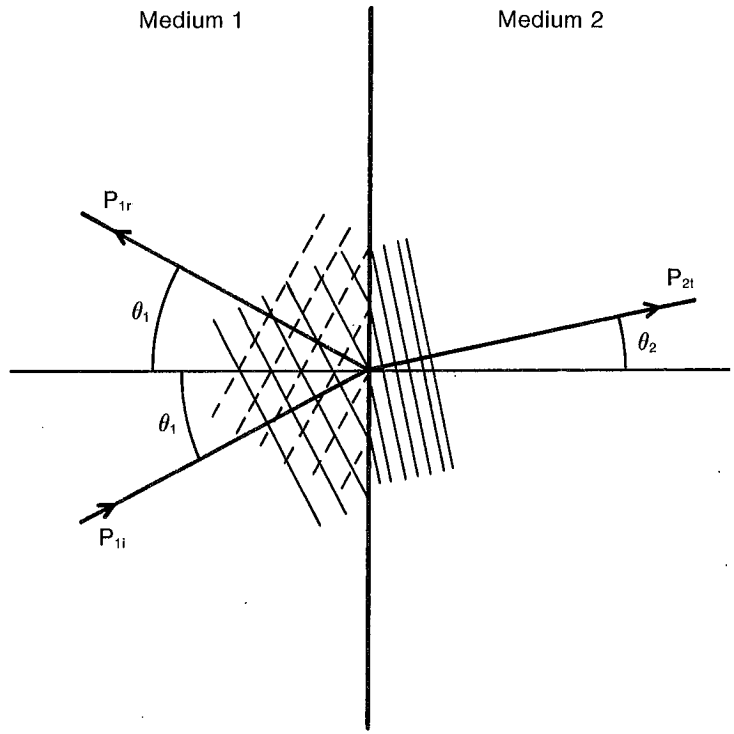

Fig. 8.4. Wave in Medium 1 incident at an angle θ_1, with respect to the normal to the interface between two media. No energy returned to the interface in Medium 2 and no absorption within media.

$$R_P = \frac{r_{21} - \dfrac{\cos\theta_2}{\cos\theta_1}}{r_{21} + \dfrac{\cos\theta_2}{\cos\theta_1}} \tag{21}$$

$$T_P = \frac{2r_{21}}{r_{21} + \dfrac{\cos\theta_2}{\cos\theta_1}} \tag{22}$$

$$R_I = R_P{}^2 = \frac{\left(r_{21} - \dfrac{\cos\theta_2}{\cos\theta_1}\right)^2}{\left(r_{21} + \dfrac{\cos\theta_2}{\cos\theta_1}\right)^2} \tag{23}$$

$$T_I = \frac{4r_{21}}{\left(r_{21} + \dfrac{\cos\theta_2}{\cos\theta_1}\right)^2} \qquad (24)$$

If $\sin\theta_1 > (c_1/c_2)$, the incident wave is totally reflected, and there is no propagation of a reflected wave in Medium 2.

Case 4: This case is very similar to that of Case 3 except that the two media are considered to be viscoelastic solids capable of propagating transverse (shear) waves. Shear waves (waves with particle displacement perpendicular to the direction of propagation) may exist in solids or very viscous liquids. A longitudinal wave incident on an interface between two such materials will generate reflected and refracted shear waves in addition to longitudinal waves, *i.e.*, mode conversion from longitudinal waves to shear waves occurs (see Figure 8.5). The angles are defined in terms of the appropriate velocities and the angle of incidence θ_1 as follows:

$$\sin\theta_2 = \frac{c_{2L}}{c_{1L}}\sin\theta_1 \qquad (25a)$$

$$\sin\beta_1 = \frac{c_{1S}}{c_{1L}}\sin\theta_1 \qquad (25b)$$

$$\sin\beta_2 = \frac{c_{2S}}{c_{2L}}\sin\theta_1 \qquad (25c)$$

where c_{1L} and c_{1S} are the longitudinal and shear velocities in Medium 1, and c_{2L} and c_{2S} are the longitudinal and shear velocities in Medium 2. If $\sin\theta_1 > (c_{1L}/c_{2L})$, there is no transmitted longitudinal wave. Further, if $\sin\theta_1 > (c_{1L}/c_{2S})$, there is no transmitted shear wave, *i.e.*, neither wave is transmitted since $c_{2L} > c_{2S}$ is always true. Since the reflection and transmission coefficients for each wave are quite complex, further discussion of mode conversion is delayed until later, where related heating phenomena are discussed.

DIFFRACTION AND BEAM PROFILES

In the previous sections only the idealized case of plane wave propagation was considered. The acoustic field distribution from a real source will approximate a plane wave in very limited regions only. In general, it will be a rather complex distribution depending on a) the dimensions of the radiator relative to the wavelength of sound in the transmitting medium; b) the shape of the radiator; c) the displacement amplitude distribution over the surface of the radiator; and d) the acoustic absorption coefficient of the medium at the frequency of the acoustic field. The acoustic field produced by non-focusing sources is considered in this section; focusing is discussed separately in the next section.

It is convenient to discuss acoustic fields produced by non-focusing radiators by considering first the field near the radiator (the Fresnel region) and then the far field (the Fraunhofer region) (1). The dependence of the

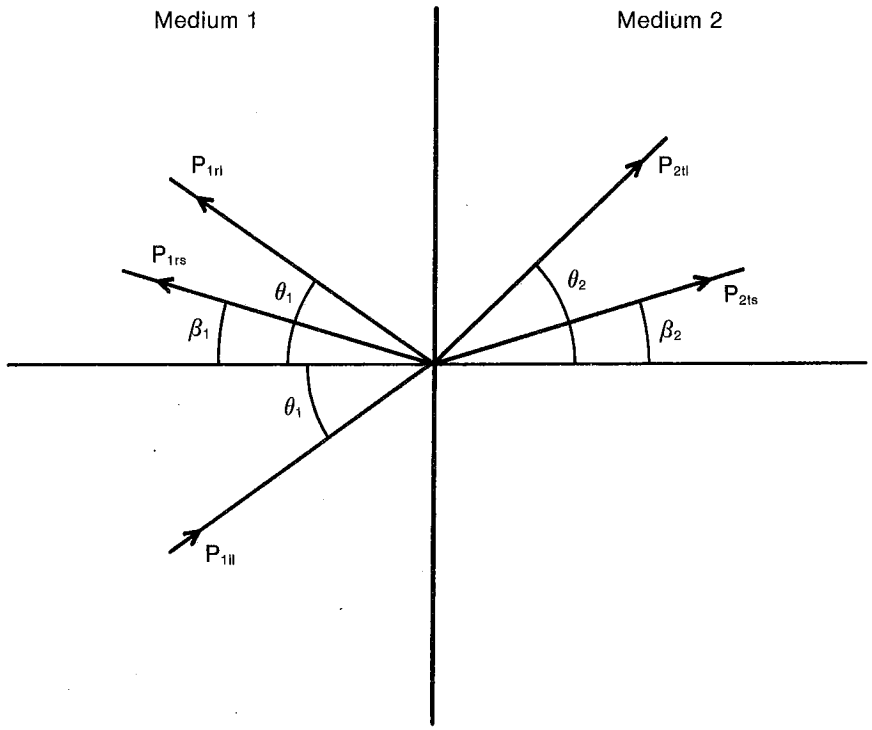

Fig. 8.5. Wave in Medium 1 incident at angle θ_1 with respect to the normal to the interface between two viscoelastic solids. Both shear waves and longitudinal waves are reflected and refracted.

field configuration on the factors listed previously is illustrated by discussing the fields produced by plane circular vibrating surfaces. The formulas given can be used to estimate the effects of varying the dimensional parameters.

The Near Field

The near field, or Fresnel region, distribution exhibits a number of maxima and minima along the axis of the radiator (1). The positions and amplitudes of these depend greatly on the velocity amplitude distribution over the source and on the ratio of source diameter to wavelength.

Figure 8.6 shows, for a plane circular vibrating element, the calculated axial field distribution of the near field for a 6.67 ratio of radius a to wavelength λ. The velocity amplitude distribution is uniform over the radiating element, and the vibrating surface is at $x/a = 0$. At distances beyond the farthest maximum, the pressure amplitude decreases monotonically and inversely with the distance from the vibrating surface. The extent of the near field and the number of maxima and minima along the axis are determined by the quantity a/λ. If $a/\lambda \gg 1$, the distance to the maximum

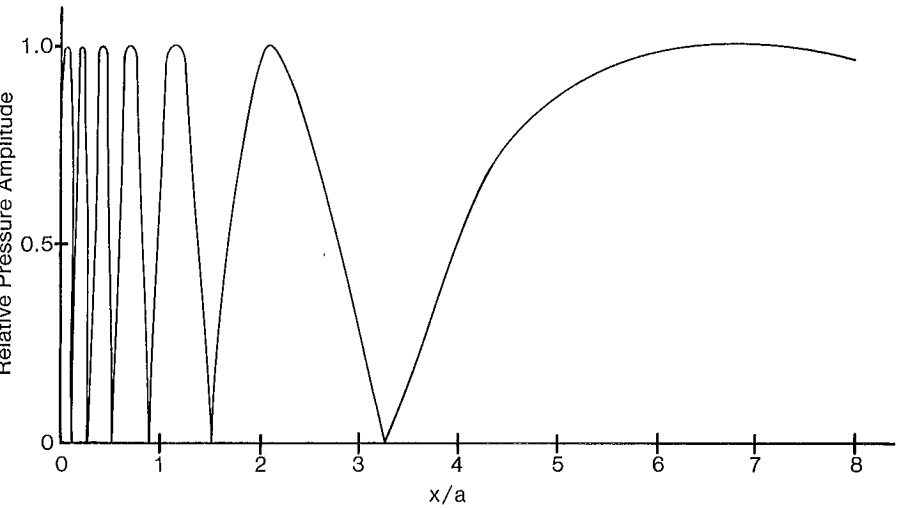

Fig. 8.6. Axial pressure amplitude distribution in the near field produced by a uniformly vibrating plane circular element.

farthest from the vibrating surface is given by

$$(X_0)_{max} = \frac{a^2}{\lambda} \tag{26}$$

The quantity $(X_0)_{max}$ is the distance from the face of the radiator to the point where the transition from near to far field approximately occurs, the last axial maximum. The number of maxima N in the near field can be obtained from

$$\frac{a}{\lambda} + \frac{1}{2} > N \tag{27}$$

That is, N is the nearest integer which is less than the numerical value of the left hand term of this equation. It should be noted that when $a/\lambda \gg 1$, the extent (in radii of the element) and number of maxima in the near field region are both nearly equal to the number of wavelengths of sound contained in the radius of the vibrating element exposed to the medium. The distance between adjacent maxima or minima decreases as one moves from the transition region toward the radiating element. It is clear from Equations *26* and *27* that for any element, as the operating frequency increases (the wavelength in the medium decreases), the distance to the transition to the far field recedes farther from the radiating element, and the number of extrema (maxima and minima) increases. These changes are proportional to the first power of the frequency.

The field distribution normal to the axis of the beam also exhibits a fairly complex structure in the near field. The number of extrema in the transverse

field pattern changes with position along the axis of the beam (2). Such pattern shifts occur in increments of distance along the axis corresponding to positions of adjacent extrema.

When non-uniform vibration amplitude distributions exist over the radiating face of the element, some shifting of the positions of the various extrema in the near field occurs. Drastic modifications of the amplitude of the swing from maximum to minimum of the extrema also occur (2). The position of the last axial maximum and the number of extrema, however, are still given approximately by Equations *26* and *27*. Instead of the constant amplitude shown in Figure 8.6, the axial field distribution exhibits swing amplitudes which are completely different in magnitude for some extrema. An interesting feature of non-uniform amplitude distributions is that the ratios of maxima to minima in the axial distribution are not nearly as large as with uniform distributions. Thus, by appropriate choice of amplitude distribution, it is possible to "flatten out" the axial distribution over a considerable distance (2).

If the medium has an acoustic absorption coefficient sufficiently large at the frequency of the field such that an appreciable fraction of the acoustic energy is absorbed in traversing the distance from the element to the position in the near field under attention, then the swing of the extrema at that position is modified compared with that characteristic of the field produced in a non-absorbing medium having the same value of the sound velocity. This effect increases in importance as the frequency increases, since the absorption per unit path length increases with frequency.

The Far Field

The far field, or Fraunhofer region, may be considered to begin at the position of the last axial maximum of the near field (see Equation *26*). Beyond this position, the axial acoustic pressure amplitude varies inversely with the distance from the source; the intensity varies as the inverse square of the distance; and the cross section of the acoustic beam increases.

Figure 8.7 provides a useful though very simplified representation of the field from a circular source with a uniform velocity amplitude distribution. The near field is shown as a region of uniform cross-section, whereas the cross-section in the far field increases with distance from the source.

The structure of the far field for a circular source, having a uniform velocity amplitude distribution, can be described more completely in terms of the pressure amplitude as follows (1)

$$|p| = \left(\frac{P}{x}\right) \left| \frac{2J_1\left(\frac{2\pi a}{\lambda}\sin\phi\right)}{\frac{2\pi a}{\lambda}\sin\phi} \right| \tag{28}$$

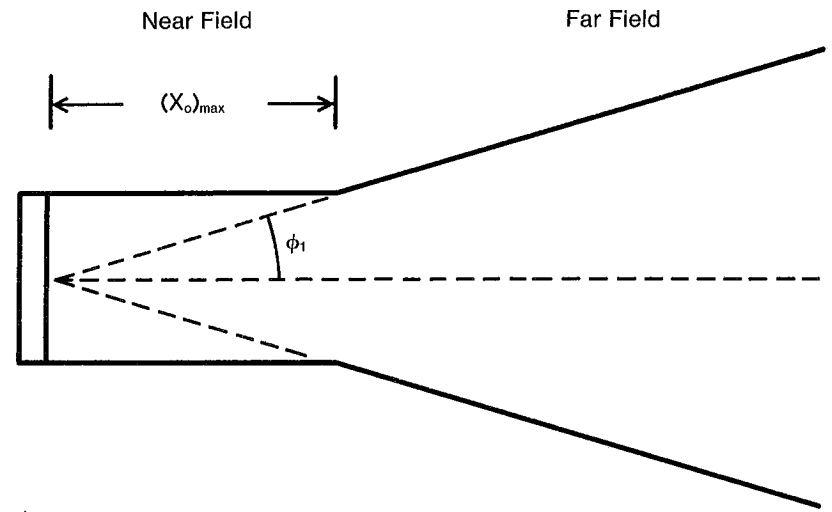

g. 8.7. Conception of field distribution for a circular source with uniform velocity amplitude distribution.

he first factor of this expression describes the decrease in pressure amplide which occurs with increasing distance from the source. The second ctor, in which J_1 designates the Bessel function of the first kind of order he (3) and ϕ is the azimuth angle measured from the axis of the radiating ement, describes the angular width of the beam and the number and agnitude of the side lobes. This is called the directivity function and is own graphically in Figure 8.8. For a radiator of a specified radius operating a fixed frequency, there exists a minimum angular width of the main eam which cannot be reduced regardless of the vibration amplitude distriution over the radiating surface. The radius of the source (measured in avelengths) affects the width of the main beam and the number of the de lobes (2). The minimum width of the main beam, as measured between he zeros on either side (which can be derived from Equation *28*), is given

$$\sin \phi_1 = 0.61 \frac{\lambda}{a} \qquad (29)$$

here ϕ_1 is the half-width, in angular measure, of the beam (see Figure 8.7). If the vibration amplitude is non-uniformly distributed ("shading" of the bration amplitude) over the radiator face, the beam characteristics can be eatly altered (2). That is, the amplitudes of one or more side lobes can be ecreased; however, the width of the main beam increases.

FOCUSING

Ultrasonic waves can be focused, according to the same principles as light aves, allowing for higher concentrations of energy, narrower beams, and

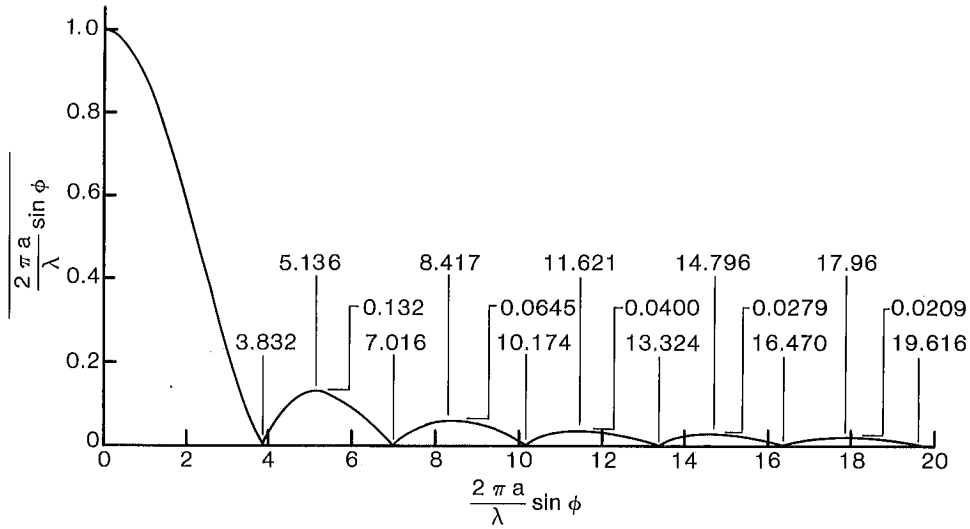

Fig. 8.8. Directivity function for a circular source with a uniform velocity amplitude distribution. See Equation *28*.

control of field distributions as the experimenter wishes. This allows small, circumscribed volumes of tissue to be treated hyperthermically (4). Various types of focusing techniques are available including lens, formed vibrating element, and electronic focusing systems. Reflector focusing systems have also been used in the past (5).

Lens Focusing Systems

A typical lens focusing system is shown in Figure 8.9, consisting of a piezoelectric vibrating element which may be directly bonded to the lens, or separated from it by an appropriate thickness of acoustic coupling material. Other lens focusing systems might consist of an array of vibrating elements with a single lens, or might use several of the systems pictured in Figure 8.9, all arranged to have a common focal region. Since solids are commonly used in fabricating lenses for precision transducers, and since the velocity of sound in most solids is greater than that in water or in non-mineralized physiological media, the lens shape is plano-concave. The index of refraction n (n = speed of sound in lens material/speed of sound in propagating medium) of the lens material, relative to the medium of interest, is greater than unity so that plane waves incident normally on the plane surface of the lens are refracted toward the principal axis when emerging at the concave surface and thus, for a properly shaped lens, are brought to a focus. Referring to Figure 8.9*a*, the focal length F of the lens is defined as the distance from the point on the curved surface on the axis to the midpoint of the region of convergence (*i.e.*, the center of the focal region). The working distance H is the distance from the plane containing the peripheral boundary

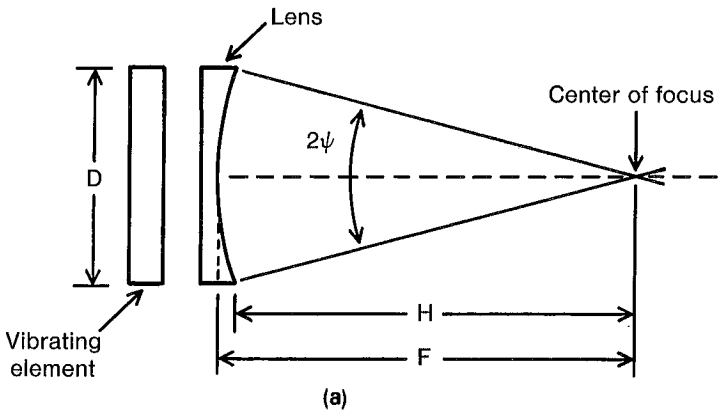

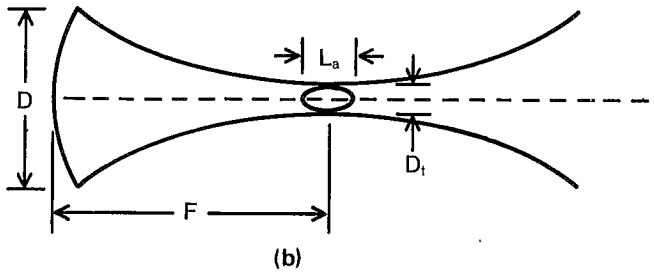

Fig. 8.9. (*a*) Schematic diagram of acoustic lens focusing system. (*b*) Illustration of the focal region of the lens.

of the curved surface of the lens to the center of the focal region. In many cases, this distance is the maximum working depth for the radiation of biological systems, since these systems are in general too large to be brought into the region bounded by the peripheral plane and the concave surface. The aperture angle 2ψ (hereafter referred to as simply the aperture) of the lens is the angle of the right cone with its apex at the center of the focal region and an altitude equal to the working distance.

If R designates the radius of curvature of the concave surface of a spherical lens of small aperture, the focal length F is

$$F \simeq \frac{R}{1-(1/n)} \qquad (30)$$

where it is assumed that the aperture D is small and that the angles of incidence and refraction are small enough so that the sine function can be approximated by the tangent function. The working distance H is given by

$$H \simeq F\left(1-\frac{F\tan^2\psi}{2R}\right) \qquad (31)$$

Large aperture lens systems may be designed using elliptical refracting surfaces (5).

The design of lens focusing systems requires knowledge of the relationships between the dimensions of the focal region, which depend on the wavelength of sound in the medium and on the lens parameters. The size and shape of the focal region determine the *minimum* volume of material which can be irradiated and the geometric shape which can be treated without affecting surrounding structures. It is convenient to describe the size of the focal region in terms of a transverse diameter and an axial length (see Figure 8.9*b*). The transverse diameter D_t is the distance across the focal region, perpendicular to the direction of propagation, at which the intensity of the acoustic field is reduced to one half the peak value. It may be expressed as

$$D_t \simeq q_t\,(F/D)\lambda \qquad (32)$$

where D is the diameter of the lens (as shown in Figure 8.9*b*), F is the focal length, and λ is the wavelength in the medium. The quantity q_t is dimensionless and depends somewhat on the half-aperture angle ψ. For values of $\psi \leq 50°$, an average value of q_t which permits calculation of D_t to within about 20 percent, is 1.0. Similarly, the axial length L_a of the focal region, the distance between points along the direction of propagation at which the intensity is reduced to one-half the peak value, is given by

$$L_a \simeq q_a D_t \qquad (33)$$

The quantity q_a depends on the half-aperture angle ψ as shown in Figure 8.10. From Equation *33* and Figure 8.10, it can be seen that the ratio of axial length to transverse diameter decreases as the aperture angle increases. Further, since q_a is always greater than unity, the focal region will always be ellipsoid-like with its major axis along the axis of the sound beam.

The gain of the lens is defined as the ratio of the intensity at the center of the focal region I_F to that at the surface of the lens in contact with the medium I_o when the lens is driven uniformly. This lens gain G_1 can be expressed for lenses with small aperture angles ($2\psi \leq 38°$) approximately in terms of the lens diameter and the transverse diameter of the focal region as

$$G_1 = I_F/I_o \simeq 0.8(D/D_t)^2 \qquad (34)$$

The spacing between the vibrating element and the lens, and the change in thickness of the lens material, modify the total gain of the lens system (5,6).

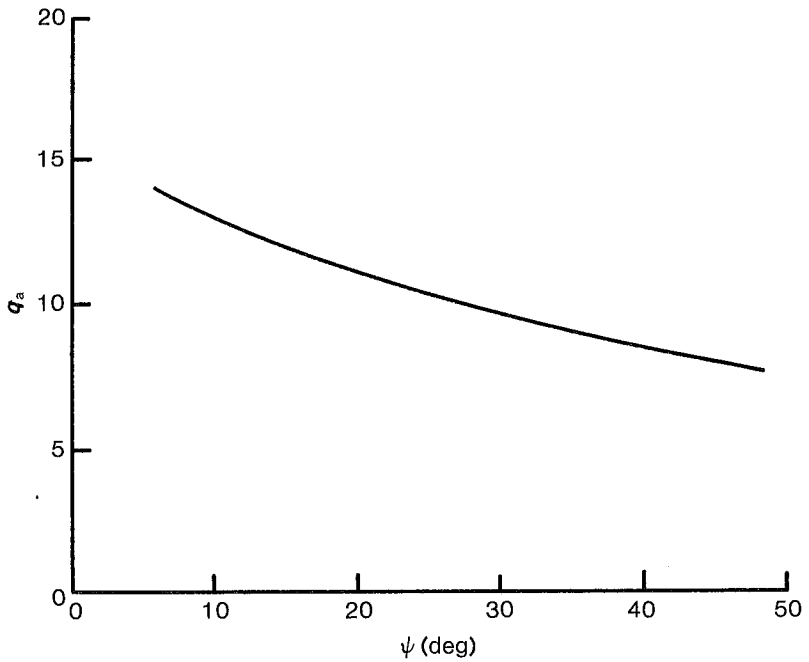

Fig. 8.10. The dimensionless lens parameter q_a versus the half-aperture angle Ψ.

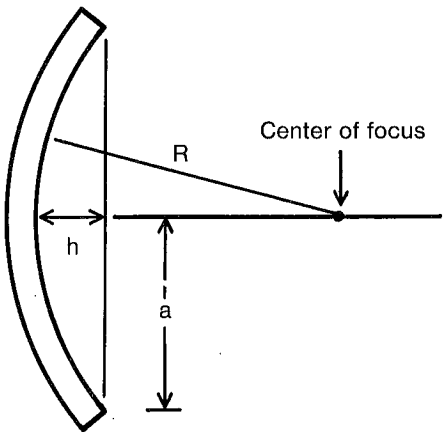

Fig. 8.11. Schematic of a section of a spherical shell used as a focusing transducer.

Formed Focusing Systems

Curved or "bowl"-shaped focusing systems can be fabricated from polycrystalline materials by casting ceramic material into the desired shape and then polarizing the material. If the concave surface is spherical, the transducer may be called a spherical shell, and the sound wave produced will converge to a focus (see Figure 8.11). The focal region is located near the

center of curvature of the shell, and is closer to the exact center for larger values of h/λ, where h is the depth of the shell (2). The lateral width D_t of the focal region is expressed as

$$D_t \simeq 1.22 \frac{R\lambda}{a} \tag{35}$$

where a is the radius of the disk and R is the radius of curvature (2,7), see Figure 8.11. The gain of this system is given by

$$G = \frac{I_F}{I_o} \simeq \left(\frac{2\pi h}{\lambda}\right)^2 \tag{36}$$

where I_F is the intensity at the focus and I_o is the intensity at the shell surface (2,7).

Electronic Focusing Systems

Both one- and two-dimensional arrays of piezoelectric elements may be used, with varied delays of the electrical signal to the elements, to achieve dynamic focusing (8). This principle is illustrated for a linear array in Figure 8.12 where the delay to each element is adjusted so that the signals reach a common point at distance F on axis at the same time, *i.e.*, the system focuses at this point. By changing the delays, the focal region may be moved in range and azimuth. A two-dimensional array of elements would allow movement of the focus in three dimensions.

Another common type of electronic focusing system consists of an annular

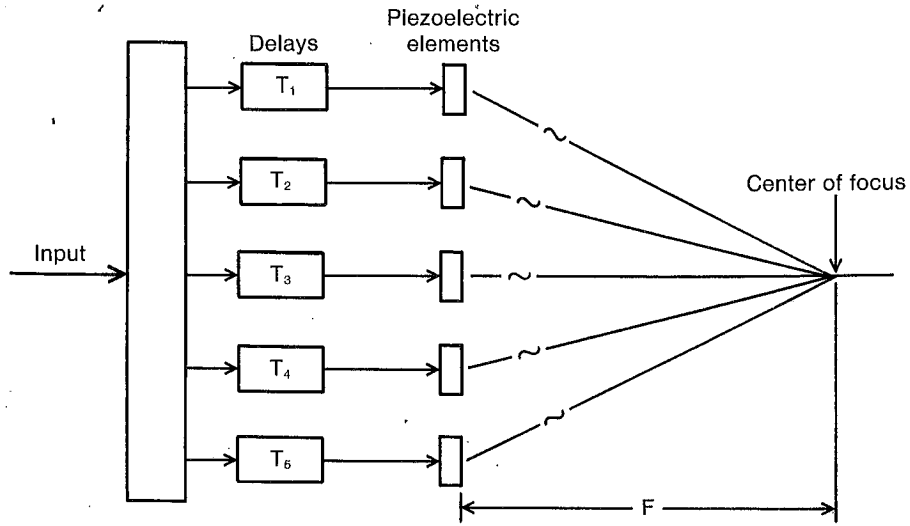

Fig. 8.12. Linear array with electrical delays adjusted for on axis focus at focal distance F.

array which can be formed by creating an annular electrode pattern on a piezoelectric element or by using separate elements as illustrated in Figure 8.13. This allows movement of the focal region along the transducer axis. The transverse dimension of the focal region of an annular array is given by an equation similar to Equation *35*, where a is the radius of the active portion of the array and R is the focal length. The aperture of any of the electronic focusing systems may be varied to adjust the dimensions of the focal region, *i.e.*, the larger the aperture the smaller the focal dimensions.

Comparing the various focusing systems, plastic materials such as plexiglass possess appropriate values for the speed of sound and impedance to focus sound into water, but they also have appreciable absorption coefficients and are subject to failure at high continuous power levels. The ceramic shell represents a convenient focusing system since it is compact and free from the problems associated with lens systems. Since the shells are formed from ceramic materials, however, they may suffer from failure at high acoustic outputs, and their response may change over long periods of time. The electronic or dynamic focusing systems provide a means of changing focal position and size, but suffer from the need for much more complex electronic driving circuitry and for complex mechanical mounting of the elements into an array.

Instrumentation

This section provides basic information about sources of ultrasound, various receivers, and measurement devices. The discussion of sources ignores radio frequency electrical drive circuitry, but covers the fundamentals of piezoelectric elements which convert electrical energy into acoustical energy (and vice versa). A number of measurement methods which are used to determine ultrasonic field distributions and to determine the absolute magnitude of the acoustic power and/or energy flux from a given source are discussed.

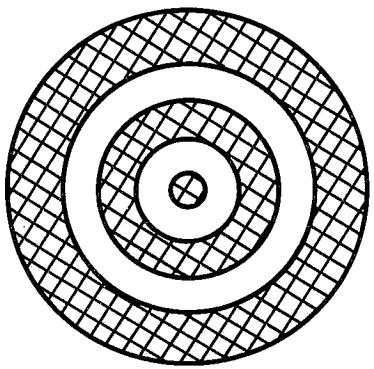

Fig. 8.13. Arrangement of active elements to form an annular array.

SOURCES, PIEZOELECTRIC ELEMENTS

Materials which exhibit the piezoelectric effect are used to generate continuous ultrasonic waves for therapeutic applications. It is the inverse piezoelectric effect which describes the linear relationship between the change in geometry of the material and the applied electric field (see Figure 8.14). A disk of a piezoelectric material of proper crystallographic orientation will change its thickness when a voltage is applied to the electrodes on the faces of the disk. The inverse piezoelectric effect, in this example, manifests itself as relative motion of the two disk faces toward and away from each other in response to the applied alternating voltage. Thus, a material in contact with one of these oscillating faces experiences a periodic disturbance which propagates away from the face at the speed of sound in that medium. The frequency of the ultrasonic wave propagating in the medium is the same as the frequency of the applied sinusoidal voltage. For a useful output, however, this frequency must correspond to one of the resonant frequencies f_n of the transducer given by

$$f_n = n\frac{c}{2d} \qquad n = 1,3,5,7,\ldots \tag{37}$$

where d is the thickness of the disk, and c is the ultrasonic velocity in the transducer material. Equation *37* can be rearranged to give the thickness

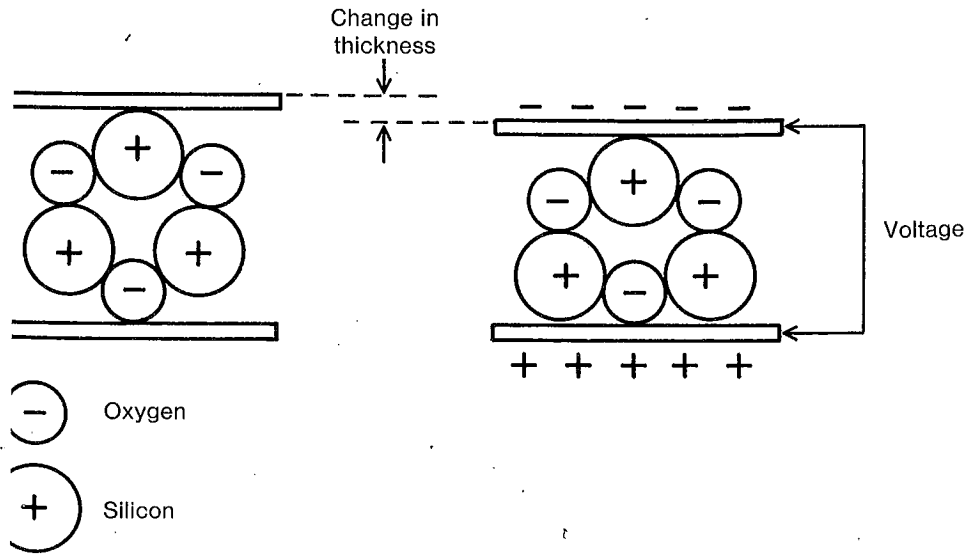

Fig. 8.14. Schematic representation of the piezoelectric effect in quartz. The change in thickness of a disk is related to the voltage between its faces.

for a given resonance frequency as

$$d = n\frac{c}{2f_n} = n\frac{\lambda_n}{2} \qquad (38)$$

where λ_n is the wavelength in the transducer material at the frequency f_n. It is apparent that the resonant thicknesses are equal to odd multiples of a half-wavelength, though the first resonant or fundamental frequency is generally used for efficient and convenient operation. As a sample calculation, a PZT-4 ceramic disk can be cut to a thickness of 2.0 mm (c = 4000 m/s) for a fundamental resonant frequency of 1 MHz. Although several natural piezoelectric materials exist and are used in ultrasonic applications, the typical therapeutic unit uses transducers of polycrystalline ceramic materials. These materials are formed into appropriate shapes, *e.g.*, a disk, and are then polarized to make them piezoelectric. These piezoelectric ceramics have been formulated to provide stronger coupling of the electrical and acoustical energies than is provided by natural crystals such as quartz. Although they have high internal losses compared to quartz, they are also more convenient to use since they may be excited with lower driving voltages. The amount of energy radiated from the transducer depends upon the properties of the transducer material, the loading material (the material into which the energy is radiated), any loading applied to the back of the transducer, and the losses within the transducer material itself.

MEASUREMENT METHODS

For effective application of therapeutic ultrasound, it is important to know the beam profile of the source and the peak intensity and/or total acoustic power output over the range of output level adjustment. Figure 8.15 shows a typical intensity profile transverse to the transducer axis. From such a distribution and knowledge of the attenuation characteristics, absorption coefficients and thermal properties of tissue, it is possible to determine the heating rate at various locations within a specimen. The following four methods have been found to be very effective in providing the above information under free field conditions:

Piezoelectric Probe

A piezoelectric probe is fabricated from a piezoelectric material, usually a ceramic material, and uses the direct piezoelectric effect to convert the mechanical energy of the acoustic wave into electrical energy for measurement. Such probes produce a voltage output proportional to the acoustic pressure on a surface(s) (see Figure 8.16). Provided that it has dimensions which are small compared to the distances over which significant changes in the pressure field occur, the hydrophone probe (so called because it is used to detect sound underwater) may be used to determine the relative

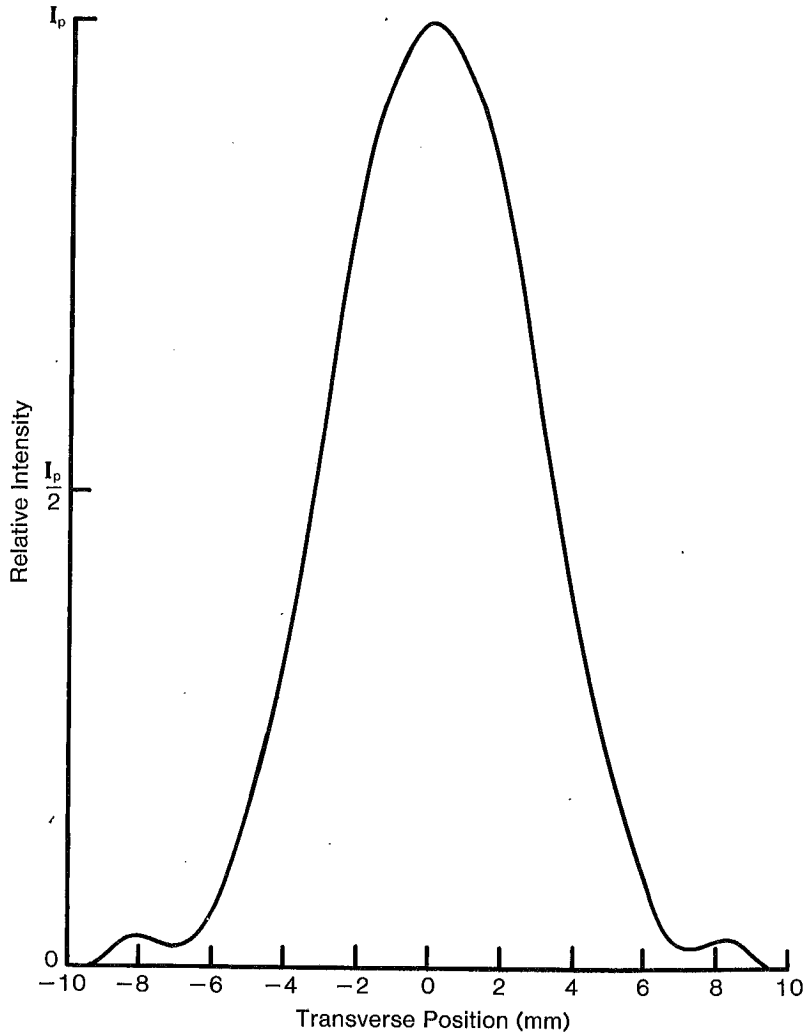

Fig. 8.15. Sample plot of the intensity profile transverse to the direction of propagation in the far field of a circular source.

pressure distribution of a source. If such a probe is calibrated, it can be used to determine the pressure amplitude in a field directly; and assuming a plane wave field, the intensity distribution can be calculated (see Table 8.1).

Transient Thermoelectric Probe

A transient thermoelectric probe consists of a small diameter thermocouple junction embedded in an absorbing material. The absorbing material converts a portion of the incident acoustical energy into heat, causing a

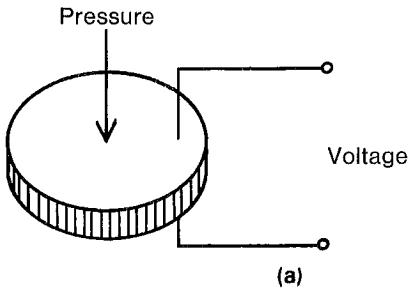

(a)

Fig. 8.16. Piezoelectric transducer elements: (*a*) disk. (*b*) section of cyclindrical probe.

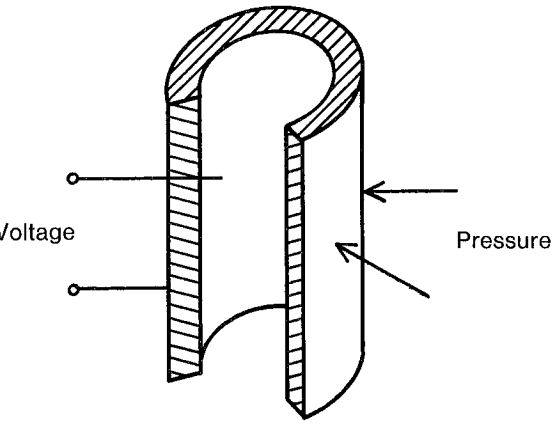

(b)

temperature rise at a rate which is given by

$$\left(\frac{dT}{dt}\right)_o = \frac{2\alpha I}{\rho C_p} \qquad (39)$$

where $\left(\frac{dT}{dt}\right)_o$ is the initial rate of temperature rise (*i.e.*, before diffusion becomes significant), α is the absorption coefficient, I is the acoustic intensity, and ρC_p is the product of the material density and its heat capacity-at constant pressure. This initial rate of temperature rise can be determined experimentally by monitoring the emf output of the embedded thermocouple. If α and ρC_p are known for the embedding material, the intensity at the thermocouple junction can be determined in an absolute manner at points of interest within the field by Equation *39*. If these properties are not known, the probe can be calibrated by another standard absolute method or can simply be used to determine relative intensity levels.

A number of factors affect the observed temperature rise dT of Equation *39*. In the presence of an acoustic wave, relative motion occurs between the thermocouple wire and the surrounding medium, producing heating in addition to that from absorption. This additional viscous heating tends toward an equilibrium value in a short time (on the order of 0.1 to 0.3 seconds) and can be minimized by making the thermocouple wire very small in diameter. Thus, for small wire sizes (on the order of 15 μm diameter or less), the rate of temperature rise may be determined from the slope of the thermal emf at approximately 0.5 seconds after the sound is turned on. The accuracy of Equation *39* is also reduced by any diffusion of heat toward or away from the point of measurement. The importance to this technique of heat diffusion and other artifacts has been discussed previously (9–12). Since the thermocouple wire and junction are small compared to distances over which field variations occur, and are in fact small compared to a wavelength, this probe may be used to measure the fine detail of an ultrasonic field.

Radiation Force Power Meter

The two methods just discussed are used to determine pressure or intensity at various points in an acoustic field. On the other hand, a radiation force power detector may be used to determine the total acoustic power output, which is the integrated intensity over the entire beam area. A knowledge of the relative beam profile, such as that shown in Figure 8.15, would allow the total acoustic power to be calculated from the absolute intensity at one point, or vice versa, the absolute intensity at any point to be calculated from the total acoustic power.

A radiation force power detector simply measures the force exerted on a target by a sound beam. This may be accomplished using various mechanical systems or electromechanical balances. The force (F_r) per unit area on a given target (*i.e.*, the radiation pressure P_r) can be expressed as

$$P_r = GE = G\left(\frac{I}{c}\right) \qquad (40)$$

where E is the energy density given as I/c, and G is a parameter which depends on the target type and physical configuration (7) as shown in Table 8.3. The force exerted on a target large compared to the sound beam is the integration (summation) of the radiation pressure (related to the intensity by Equation *40*) over the beam. The average intensity I_{ave} in a beam of known cross-section A (often taken as the transducer area) can be determined from the measurement of the force F_r. In this case, the average

8.3. *The Constant G of Equation 40 for Various Physical Configurations*

Physical Configuration	G
absorber, normal incidence	1
reflector, normal incidence	2
reflector, incident at angle θ_1 to surface normal	$2\cos^2\theta_1$

on pressure would be expressed as

$$P_{r_{ave}} = \frac{F_r}{A} \tag{41}$$

Equation *40*, the average intensity is given by

$$I_{ave} = \frac{c}{G} P_{r_{ave}} = \frac{c}{G}\frac{F_r}{A} \tag{42}$$

mple, if the force from a source of cross-sectional area 5 cm^2 on a absorber in water at 37°C was measured to be 0.01 Newtons, the intensity of the acoustic field producing the force was 3 W/cm^2.

average intensity I_{ave} is equal to the integration of the intensity tion transverse to the beam divided by the area of the field:

$$I_{ave} = \frac{2\pi \int_o^{x_o} \mathrm{I(x)\ x\ dx}}{\mathrm{A}} \tag{43}$$

$I(x)$ is the intensity as a function of distance off axis x, and x_o is the the lateral extent of the beam. For example, if $I(x) = I_p(1 - 7x^2)$ I_p is the peak intensity, then for $x_0 = 0.4$ cm

$$I_{ave} = \frac{2\pi I_p \int_0^{0.4} (1 - 7x^2)\ x\ dx}{\pi(0.4)^2} = 0.44\ I_p \tag{44}$$

adiometer

radiation force exerted on a small sphere suspended in an ultrasonic used as an absolute measure of the intensity averaged over the cross of the sphere. The sphere is typically made of a rigid material such less steel, *i.e.*, a stainless steel ball bearing, and can be small (1 mm er or less) compared to the distance for field variations. This tech- s an absolute method for determining intensities, and requires no s calibration.

teel ball of a typical radiometer is suspended by a bifilar arrangement small diameter nylon monofilament. The radiation force F_r deflects ere; the magnitude of the deflection d permits evaluation of the force

exerted by the ultrasonic irradiation field according to

$$F_r = \frac{\mathrm{mgd}}{(L^2 - d^2)^{1/2}} \tag{45}$$

where L is the length of the suspension; m is the mass of the sphere plus the mass of the suspension structure involved, both corrected for buoyancy; and g is the gravitational constant (see Figure 8.17). The intensity is related to the force by

$$I = \frac{F_r c}{\pi a^2 Y} \tag{46}$$

where a is the radius of the sphere; c is the speed of sound in the fluid medium; and the dimensionless quantity Y is known as the acoustic radiation force function. This function is known to have a complex dependence on the ratio of the wavelength in the fluid to the ball radius. For accurate determination of intensity, the rather detailed plots of this function for 440C stainless steel have been published (13). As an example, consider a 1/16 inch diameter ($a = 0.79$ mm) stainless steel (440 C) ball suspended in water and

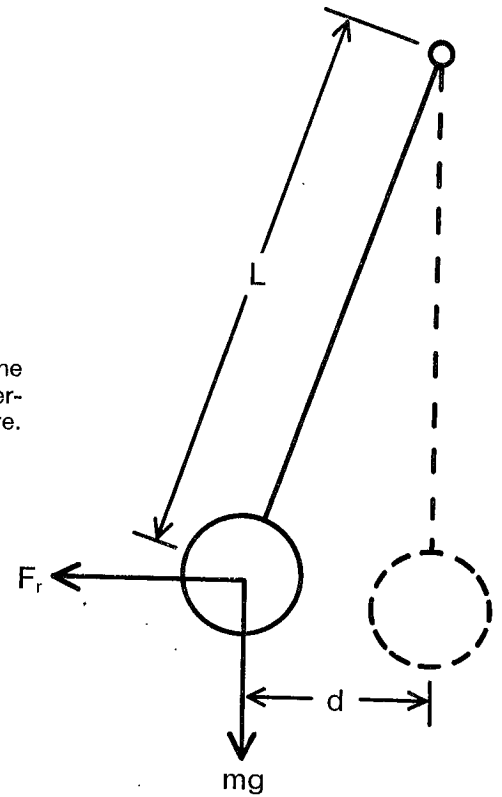

Fig. 8.17. Schematic illustration of the experimental arrangement for determining the radiation force on a sphere.

xposed to 1 MHz sound. For this case, $Y = 0.886$ such that for $d = 1$ cm, $= 0.0133$ gm, $L = 11$ cm and $c = 1500$ m/s, an intensity of approximately W/cm^2 is calculated.

Propagation in and Interaction with Tissues

A knowledge of the propagation properties of ultrasound in tissues and of ne interaction of ultrasound with tissues are both fundamental to the safe nd effective use of therapeutic ultrasound.

PROPAGATION PROPERTIES OF ULTRASOUND IN TISSUES

A substantial body of literature is available which reports results of ltrasonic propagation property measurements in tissues (14–16). However, he usefulness of these measurements to clinical applications is limited ecause most of them were not made in freshly excised tissues, the temperatures varied over a broad range, the conditions of measurement were not lways specified, and the bulk of the measurements were made in the same mited number of tissues (17). These limitations exist in part because neasurements are often made to gain a basic understanding of the interaction between ultrasound and tissues, rather than to provide data for development of, and application to, clinical instrumentation.

As is evident from the two earlier parts of this chapter, the propagation arameters of interest include the speed of propagation (velocity), the ttenuation coefficient, the absorption coefficient, and the characteristic mpedance. Table 8.4 contains a listing, ordered by increasing attenuation oefficient, of the results of measurements at 1 MHz compiled from the iterature for a few tissues relevant to therapeutic ultrasound (15, 16). The ntries in Table 8.4 represent averages over a broad range of reported neasurements. Within experimental error, the velocity and characteristic mpedance are independent of frequency. In the frequency range 0.5 to 10 MHz, the attenuation and absorption coefficients for tissues other than bone an be assumed to have a power dependence on frequency (18) expressed as

$$\alpha = \alpha_1 f^{1.1} \qquad (47)$$

where f is the frequency in MHz, α_1 is the loss coefficient (attentuation or bsorption coefficient) at 1 MHz, and α is the loss coefficient at the specified requency. Only a slight reduction in accuracy results if a linear dependence n frequency is assumed. In Table 8.4, the attenuation coefficient is specified n both decibels per centimeter and nepers per centimeter since this parameter may be used with instrument adjustments in decibels and also in the equations describing attenuation which require the attenuation coefficient n nepers per centimeter. The absorption coefficients for a number of tissues have been reported (18) and are about ⅓ to ½ of the attenuation coefficient or the same tissues. The attenuation coefficient has been found to increase vith structural protein content and with decreasing water content (19), as

TABLE 8.4. *Listing, by Increasing Attenuation Coefficient, of Propagation Properties of some Relevant Tissues at 1 MHz*

Tissue	Attenuation Coefficient $\left(\frac{dB}{cm}\right)$	Attenuation Coefficient $\left(\frac{Np}{cm}\right)$	Velocity $\left(\frac{m}{s}\right)$	Density $\left(\frac{g}{cm^3}\right)$	Impedance (10^5 rayls)	Trends
Blood	0.12	0.014	1566	1.04	1.63	Increasing structural protein content ↓ Decreasing water content
Fat	0.61	0.07	1478	0.92	1.36	
Nerve	0.88	0.10				
Muscle	1.2	0.14	1552	1.04	1.62	
Blood Vessel	1.7	0.20	153.0	1.08	1.65	
Skin	2.7	0.31	1519			
Tendon	4.9	0.56	1750			
Cartilage	5.0	0.58	1665			
Bone	13.9	1.61	3445	1.82	6.27	

indicated in Table 8.4. The speed of sound in the medium also seems to follow the same pattern. It has recently been shown that ultrasonic properties depend on the collagen and noncollagenous protein contents of tissues (20, 21). It appears that tissues of greater protein content have higher velocities and absorption coefficients, and thus, greater heating rates than tissues of lesser protein content.

INTERFACIAL HEATING

The use of ultrasound for therapeutic heating necessarily involves several tissue types or organs; thus, phenomena associated with the surfaces between tissues become important. The phenomenon of mode conversion at an interface was introduced previously, and its relevance to therapeutic ultrasound will now be considered.

The contribution to heating in bone from energy converted to the shear mode at the bone interface has been examined (22). While it was considered that shear waves do not propagate in soft tissues, bone exhibits a shear stiffness that supports the propagation of shear waves. Measurement of the shear properties of soft tissues (23), and an examination of generation of shear waves by mode conversion in these tissues (24), support these views. Since the amount of shear wave generation at an interface depends strongly on the angle of incidence, a number of angles of incidence for a fat-muscle-bone layered system have been studied (22). The results show that, for

ngles of incidence in the range 45 to 60°, the heating within the bone due o shear energy is greater than that due to energy in the longitudinal mode, ue in part to the higher absorption coefficient of the shear waves over that or longitudinal waves.

The results demonstrating additional heating due to mode conversion in ineralized tissues suggest that heating by this mechanism also may be nportant in other rigid tissues such as cartilage, although this has not yet een studied.

It is also known that increased heating occurs at interfaces in the absence f mode conversion, *e.g.*, normal incidence, when a significant amount of nergy is reflected (24). For total reflection, the heating rate is increased by factor of two for plane waves normally incident on plane interfaces.

REFERENCES

1. KINSLER, L. E. AND FREY, A. R. *Fundamentals of Acoustics.* 2nd edition, John Wiley & Sons, New York, 1962.
2. KIKUCHI, Y. Transducers for ultrasonic systems. *In: Ultrasound: Its Applications in Medicine and Biology.* Fry, F. J. (Ed). Elsevier, New York, pp. 289–342, 1978.
3. MCLACHLAN, M. W. *Bessel Functions for Engineers.* 2nd Edition, Oxford University Press, London, 1955.
4. KREMKAU, F. W. Cancer therapy with ultrasound: a historical review. *J. Clin. Ultrasound, 7:* 287–300, 1979.
5. FRY, W. J. AND DUNN, F. Ultrasound: Analysis and experimental methods in biological research. *In: Physical Techniques in Biological Research.* Nastuk, W.L. (Ed). Vol. 4. Academic Press, New York, pp. 261–394, 1962.
6. FRY, W. J. AND DUNN, F. Ultrasonic intensity gain by composite transducers. *J. Acoust. Soc. Am., 34:* 188–192, 1962.
7. HUETER, T. F. AND BOLT, R. H. *Sonics.* John Wiley & Sons, New York, 1955.
8. WELLS, P. N. T. *Biomedical Ultrasonics.* Academic Press, New York, 1977.
9. FRY, W. J. AND FRY, R. B. Determination of absolute sound levels and acoustic absorption coefficients by thermocouple probes—Theory. *J. Acoust. Soc. Am., 26:* 294–310, 1954.
10. FRY, W. J. AND FRY, R. B. Determination of absolute sound levels and acoustic absorption coefficients by thermocouple probes—Experiment. *J. Acoust. Soc. Am., 26:* 311–317, 1954.
11. GOSS, S. A., COBB, J. W. AND FRIZZELL, L. A. Effect of beam width and thermocouple size on the measurement of ultrasonic absorption using the thermoelectric technique. *1977 Ultrasonic Symposium Proceedings,* IEEE Cat. #77CH1264-1SU, pp. 206–211, 1977.
12. GOSS, S. A., FRIZZELL, L. A. AND DUNN, F. Frequency dependence of ultrasonic absorption in mammalian testis. *J. Acoust. Soc. Am., 63:* 1226–1229, 1978.
13. DUNN, F., AVERBUCH, A. J. AND O'BRIEN, W. D., JR. A primary method for the determination of ultrasonic intensity with the elastic sphere radiometer. *Acustica, 38:* 58–61, 1977.
14. CHIVERS, R. C. AND PARRY, R. J. Ultrasonic velocity and attenuation in mammalian tissues. *J. Acoust. Soc. Am., 63:* 940–953, 1978.
15. GOSS, S. A., JOHNSTON, R. L. AND DUNN, F. Comprehensive compilation of empirical ultrasonic properties of mammalian tissues. *J. Acoust. Soc. Am., 64:* 423–457, 1978.
16. GOSS, S. A., JOHNSTON, R. L. AND DUNN, F. Compilation of empirical ultrasonic properties of mammalian tissues. II. *J. Acoust. Soc. Am., 68:* 93–108, 1980.
17. GOSS, S. A., JOHNSTON, R. L. AND DUNN, F. Ultrasound mammalian tissue properties literature search. *Acoust. Lett., 1:* 171, 1978.
18. GOSS, S. A., FRIZZELL, L. A. AND DUNN, F. Ultrasonic absorption and attenuation in mammalian tissues. *Ultrasound Med. Biol., 5:* 181–186, 1979.

19. JOHNSTON, R. L., GOSS, S. A., MAYNARD, V., BRADY, J. K., FRIZZELL, L. A., O'BRIEN, W. D., JR. AND DUNN, F. Elements of tissue characterization Part I. Ultrasonic propagation properties. *In: Ultrasonic Tissue Characterization II.* Linzer, M. (Ed). National Bureau of Standards, Spec. Publ. 525, 1979.
20. O'BRIEN, W. D., JR. The role of collagen in determining ultrasonic propagation properties in tissue. *In: Acoustical Holography.* Vol. 7. Kessler, L. W. (Ed). Plenum Press, New York, pp. 37–50, 1977.
21. GOSS, S. A., FRIZZELL, L. A. AND DUNN, F. Dependence of the ultrasonic properties of biological tissue on constituent proteins. *J. Acoust. Soc. Am., 67:* 1041–1044, 1980.
22. CHAN, A. K., SIGELMANN, R. A. AND GUY, A. W. Calculations of therapeutic heat generated by ultrasound in fat-muscle-bone layers. *IEEE Trans. Biomed. Eng., BME-21:* 280–284, 1974.
23. FRIZZELL, L. A., CARSTENSEN, E. L. AND DYRO, J.F. Shear properties of mammalian tissues at low megahertz frequencies. *J. Acoust. Soc. Am., 60:* 1409–1411, 1977.
24. FRIZZELL, L. A. Ultrasonic heating of tissues. Ph.D. Thesis, University of Rochester, Rochester, N. Y., 1975. (Same as: Frizzell, L. A. and Carstensen, E. L. Ultrasonic heating of tissues. Elec. Eng. Tech. Report No. GM09933-20, University of Rochester, Rochester, NY, 1975.)